

## Effect of Annealing Time on the Power Conversion Efficiency of Silicon Nanowire Based Solar Cell Prepared by Wet Diffusion Technique

P.V. Trinh<sup>1,\*</sup>, B.H. Thang<sup>1</sup>, N.V. Chuc<sup>1,2</sup>, P.N. Hong<sup>1,2</sup>, P.N. Minh<sup>1,2,3†</sup>

<sup>1</sup> Institute of Materials Science, Vietnam Academy of Science and Technology,  
18, Hoang Quoc Viet Str., Cau Giay Distr., Hanoi, Vietnam

<sup>2</sup> Graduate University of Science and Technology, Vietnam Academy of Science and Technology,  
18, Hoang Quoc Viet Str., Cau Giay Distr., Hanoi, Vietnam

<sup>3</sup> Center for High Technology Development, Vietnam Academy of Science and Technology, 18, Hoang Quoc Viet Str.,  
Cau Giay Distr., Hanoi, Vietnam

(Received 08 September 2017; revised manuscript received 15 November 2017; published online 24 November 2017)

In this study, we present the effect of annealing time on the power conversion efficiency (PCE) of silicon nanowire (SiNW) based solar cell prepared by wet diffusion technique. P-typed SiNW arrays were prepared by metal assisted chemical etching (MACE) method using aqueous solution including HF (4.6 M) and AgNO<sub>3</sub> (0.02 M). The prepared SiNWs have V-shaped structures with the wall thickness in a range from 10-50 nm and the average length of 1.5 μm. The reflectance of SiNW array remained less than 20 % and lower compared to that of planar Si (38 %) in the range of 300-1000 nm due to the subwavelength light trapping and collective light scattering interactions. The wet diffusion technique was used to making p-n junctions in solar cell structure with different annealing time at 850 °C. The obtained results demonstrated that the PCE increases when increasing the annealing time from 30 min to 45 min then decreases with 60 min. The highest PCE obtained with cell annealed for 45 min was measured to be 2.2 % and about 2 times and 5 times higher compared to cell annealed for 60 min and 30 min, respectively. The dependence of PCE on the annealing time is attributed to the difference in the doping diffusion depth.

**Keywords:** Si nanowires, Solar cell, Power conversion efficiency, Wet diffusion, Annealing time.

DOI: [10.21272/jnep.9\(6\).06025](https://doi.org/10.21272/jnep.9(6).06025)

PACS numbers: 88.40.H, 88.40.hj

### 1. INTRODUCTION

Nowadays, the traditional energy sources such as petroleum, coal, and natural gas are being depleted off due to high usage rate and are further expected to rise in future. Development of the new alternative energy sources like solar thermal, solar electric, nuclear fission, nuclear fusion, geothermal, wind, hydroelectric and fuel from biomass is very necessary to guarantee the energy security in over the world. Among of them, the solar energy is expected to be an ideal candidate to resolve the energy problem due to possibly provide a clean and cost-effective energy source [1, 2]. Thus, research and development towards high-efficiency Silicon solar cells have been accelerating in recent years. Most of the commercial solar cell system today is based on bulk or thin film amorphous Si, however, these solar cell structure today reached to the limitation of conversion efficiency due to their limited absorption thickness. To improve the efficiency of solar cells, innovation of materials and structures are indispensable. Functionalized Silicon nanostructures have been becoming the promising candidate materials for fabricating solar cells by their special properties [3]. Using SiNWs for solar cells have been developed and investigated recently [4-6]. The obtained results demonstrated that Si wire arrays suitable for the photovoltaic devices due to offer a low reflectance and a strong broadband optical absorption [7]. Several studies have been done both theoretical and experimental studies to investigate the effects of wire diameter, length and wire pitch on the optical absorp-

tion and performance of SiNW based solar cells [8]. The studies demonstrated the radial p-n junction structure formed in individual SiNWs is optimal structure for the high-efficiency photovoltaic system [8, 9]. To form the p-n junction structure, some doping techniques such as vapor-liquid-solid (VLS), chemical vapor deposition (CVD) and wet diffusion were common used [10-15]. Therein, wet diffusion process using dopant solution shows an effective approach for lowering the cost manufacturing of solar cell [12, 15]. However, using wet diffusion technique for making p-n junction needs further optimization of various parameters such as annealing time and temperature in order to improve the performance of SiNW based solar cells.

Thus, this study is to investigate the effect of annealing time on the power conversion efficiency of SiNW based solar cell. SiNWs were prepared by MACE method then the wet diffusion technique was applied for making the p-n junction. The solar cell properties and parameters were investigated and presented.

### 2. EXPERIMENT PROCEDURE

#### 2.1 Materials

Acetone, ethanol, sulfuric acid (H<sub>2</sub>SO<sub>4</sub>), hydrogen peroxide (H<sub>2</sub>O<sub>2</sub>), hydro fluoric (HF) acid and nitric acid (HNO<sub>3</sub>) were purchased from Xilong Chemical Factory, China. Silver nitrate (AgNO<sub>3</sub>) and p-type Si (100) wafers were supplied by Sigma-Aldrich. OCD solution containing phosphorus manufactured by Tokyo Chemi-

\* [trinhpv@ims.vast.vn](mailto:trinhpv@ims.vast.vn)

† [pnminh@vast.ac.vn](mailto:pnminh@vast.ac.vn)

cal Industry Co. Silver and aluminum targets were purchased from Sigma-Aldrich for the electrode depositions.

## 2.2 Solar Cell Fabrication

SiNW arrays were prepared with an Ag-assisted etching method. p-type (100) silicon wafers were cleaned with acetone (5 min) and ethanol (5 min), rinsed with deionized water (10 min) 3 times, then immersed in a 3:1 mixture of  $H_2SO_4$  (97 %) and  $H_2O_2$  (30 %) for 10 min, thoroughly rinsed with deionized water for 10 min, and then dipped in HF solution for 1 min. The cleaned silicon wafers were immersed in an aqueous solution including HF (4.6 M) and  $AgNO_3$  (0.02 M) for 10 min at room temperature to form SiNWs. As-prepared SiNWs then rinsed in  $HNO_3$  (35 %) for 10 min to remove any residue of the silver catalyst.

To prepare the solar cell based SiNWs, firstly, SiNWs were cleaned by piranha solution for 10 min at 130 °C, followed by 2 % HF solution for 2 min to remove any native oxides. Immediately, OCD solution was spin-coated on top of the SiNW surface with speed of 2000 rpm for 60 s. After coating, a thin layer of Al film with a thickness of 500 nm was deposited on the back-side of the wafer and a finger-typed Ag-film thickness of 250 nm was deposited on the top of the wafer to form the front electrode by RF sputtering. Finally, the samples were annealed in  $N_2$  atmosphere at 850 °C by a thermal annealing system for different times of 30 min, 45 min and 60 min to prepare the solar cells.

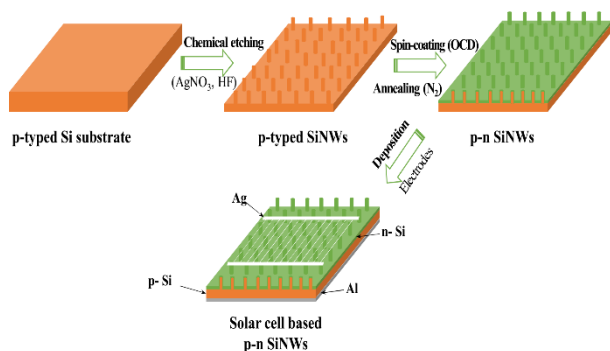


**Fig. 1** – Schematic diagram of the fabrication process of SiNWs based solar cell

## 2.3 Characterization

The morphological study was characterized by using a field emission scanning electron microscope (FESEM) Hitachi S4800. The Raman spectra were recorded using an iHR550 Jobin-Yvon spectrometer using a 514 nm laser excitation at room temperature. Optical reflectance spectra were recorded by Jacob V-570 UV/Vis/NIR spectrophotometer. The conductivity of the samples was measured by using the four-point probe method. The  $J$ - $V$  characteristics of solar cells were measured using a Keithley 2400 source meter under illumination of air mass (AM) 1.5 G with the intensity of  $100 \text{ mW}\cdot\text{cm}^{-2}$ .

## 3. RESULTS AND DISCUSSION

FESEM measurements were performed to characterize the surface structure of the SiNW arrays. Figure 2 shows the top-viewed and cross-sectional SEM images of the SiNW arrays. From top-viewed SEM images, we can see that the SiNWs were formed by the chemical etching process with high density. The prepared SiNWs were observed in V-shaped structure with the wall thickness in a range from 10-50 nm. The length of SiNWs was also determined with an average length of 1.5  $\mu\text{m}$  by cross-sectional SEM image (Figure 2d). The formation of SiNWs can be explained using the Si etching mechanism with the metal assistance reported by Huang et al. [16]. The first step, Ag nanoparticles inject holes into the Si substrate in contact positions. The second step, oxidation and etching of Si occur at the Ag/Si interface much faster compared to other position on bare Si and thus lead to nanowire formation. In this case, Ag nanoparticles act as catalytic materials help to improve the etching rate at positions with metal coverage.

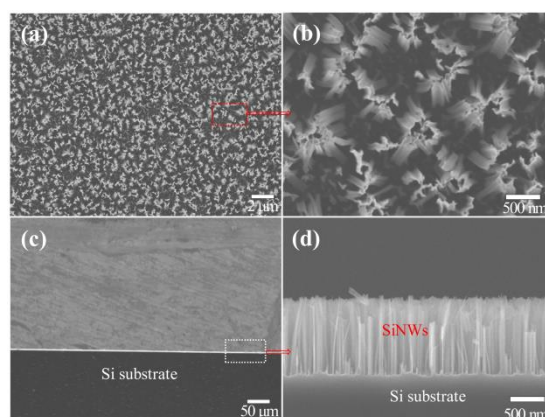


**Fig. 2** – (a-b) Top-view and (c-d) cross-sectional SEM images of SiNWs after chemical etching for 10 min

Figure 3 shows the Raman spectra of p-type Si substrate and SiNWs. As can be seen, Raman spectra of SiNWs show a peak broadening and downshift comparing with bulk Si measured in the same conditions. This could be explained using the heating effect as presented by Piscanec and coworkers [17]. According to Piscanec et al. the sensitivity of SiNW to laser heating is higher than that of bulk Si due to size effects and lower thermal conductivity. These factors will cause an inhomogeneous heating and thus lead to peak broadening [18].

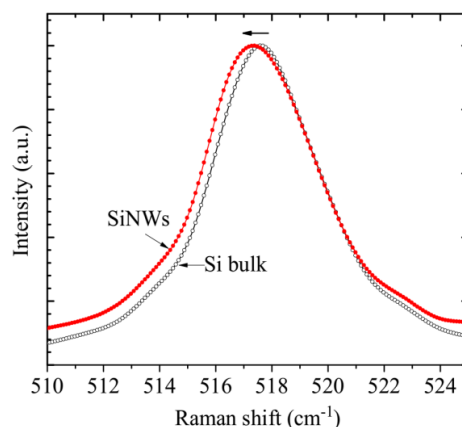


**Fig. 3** – Raman spectra of planar Si and SiNWs

Reflectance spectra in a wavelength ranging from 200 to 1000 nm of planar Si and SiNW were shown in Figure 4. As can be seen, the reflectance of SiNWs is lower than that of the planar Si substrate and remained less than 20 % compared to an average 38 % reflection of planar Si wafer in the range of 300-1000 nm. The reflectance decrease is attributed to the subwavelength light trapping and collective light scattering interactions among the densely packed SiNWs [19, 20]. In other words, the unique morphology with porosity variation from top to bottom in the arrays leading to refractive index gradient with depth and SiNW arrays in this case act as a multilayer anti-reflection surface [21].

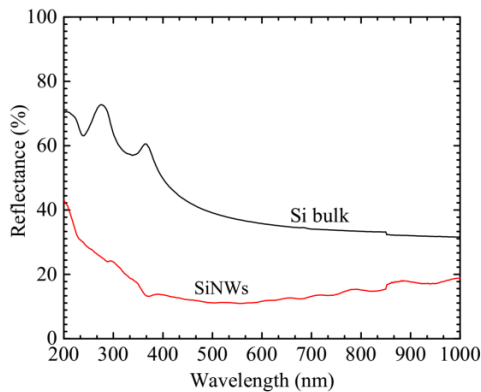


Fig. 4 – Reflectance spectra of planar Si and SiNWs

Table 1 – Solar cell parameters: short circuit current density ( $J_{sc}$ ), open circuit voltage ( $V_{oc}$ ), fill factor ( $FF$ ), efficiency ( $\eta$ ).

Cell	$J_{sc}$ (mA/cm <sup>2</sup> )	$V_{oc}$ (V)	$FF$ (%)	$\eta$ (%)
30 min	4.08	0.31	29.3	0.4
45 min	9.78	0.45	50.1	2.2
60 min	5.36	0.44	47.2	1.1

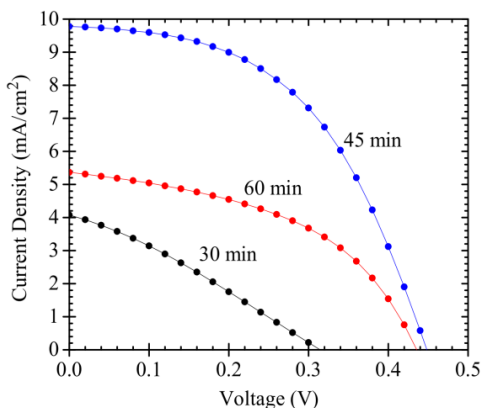


Fig. 5 – The current-voltage curves of SiNW based solar cell with different annealing times

The current-voltage curves of SiNW based solar cell with different annealing times were shown in Figure 5 and the parameters such as short circuit current density ( $J_{sc}$ ), open circuit voltage ( $V_{oc}$ ), fill factor ( $FF$ ), efficiency ( $\eta$ ) were presented in Table 1. The results indicate that the PCE increases when increasing the annealing time from 30 min to 45 min then decreases when longer annealing time was applied. The highest PCE obtained

with cell annealed for 45 min was measured to be 2.2 %. The obtained value is 2 times and 5 times higher compared to cell annealed for 60 min and 30 min, respectively. Along with the PCE, the enhancement also exhibited with other parameters such as  $J_{sc}$ ,  $V_{oc}$  and  $FF$  as presented in Table 1. The dependence of PCE on the annealing time could be explained as follow analysis. As known, the doping diffusion depth could be estimated by the equation:  $L = (D \times t)^{1/2}$ , [22] where  $D$  is the diffusivity of P into Si ( $1.5 \times 10^{-15} \text{ cm}^2\text{s}^{-1}$ ),  $t$  is the diffusion time and  $L$  is the diffusion depth. The diffusion depth for 30 min, 45 min and 60 min was calculated to be 16 nm, 20 nm and 23 nm, respectively. In addition, the flake thickness distributes in range from 20-50 nm as presented in above section. This indicated that three possibilities could be happened: (i)  $n$ -typed Si formed at few positions on SiNWs (Fig. 6a), (ii)  $n$ -typed Si formed as shell layer and coated  $p$ -typed Si core inside (Fig. 6b) and (iii)  $n$ -typed Si formed in total SiNWs (Fig. 6c). It is clear that the  $p$ - $n$  junction area is the smallest with the first possibility and resulted in the low PCE. In second possibility, the  $p$ - $n$  junction is the largest due to the formation of radial  $p$ - $n$  junction on each SiNWs. In this case, SiNWs not only reduce the reflectance but also increase the  $p$ - $n$  junction area and thus obtain the highest PCE. In third possibility, there is no radial  $p$ - $n$  junction formed, the  $p$ - $n$  junction area is decreased compared to the second possibility that will happen when the annealing time for the dopant diffusion too long and SiNWs only acted as an anti-reflection electrode and resulting in decrease of PCE.

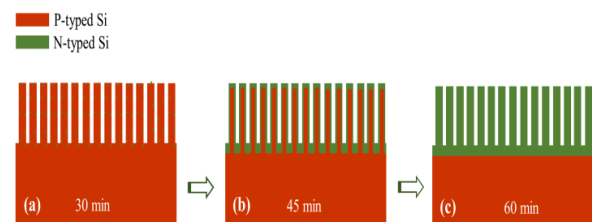


Fig. 6 – The effect of annealing time on the formation of  $p$ - $n$  junction

#### 4. CONCLUSIONS

In conclusion, V-shaped structural  $p$ -typed SiNW arrays were successfully prepared by MACE method. The reflectance of SiNW array remained less than 20 % and lower compared to that of planar Si (38 %). The  $p$ - $n$  junction in SiNW based solar cell structure was prepared using wet diffusion technique with different annealing time at 850 °C. The obtained results had shown that the PCE increases when increasing the annealing time from 30 min to 45 min then immediately decreases with 60 min. The cell annealed for 45 min has the highest PCE of 2.2 % that is 2 times and 5 times higher compared to cell annealed for 60 min and 30 min, respectively. The dependence of PCE on the annealing time is mainly due to the difference in the doping diffusion depth.

#### ACKNOWLEDGEMENT

This work was supported by the Key Laboratory for Electronic Materials and Devices, Institute of Materials Science under project CSTD 02.17.

## REFERENCES

1. P. Yadav, K. Pandey, V. Bhatt, M. Kumar, J. Kim, *Renew. Sust. Energ. Rev.* **76**, 1562 (2017).
2. M. Stuckelberger, R. Biron, N. Wyrsh, F.J. Haug, C. Ballif, *Renew. Sust. Energ. Rev.* **76**, 1497 (2017).
3. R. Yu, Q. Lin, S.F. Leung, Z. Fan, *Nano Energy* **1**, 57 (2012).
4. T. Song, S.T. Lee, B. Sun, *Nano Energy* **1**, 654 (2012).
5. Th. Stelzner, M. Pietsch, G. Andrä, F. Falk, E. Ose, S. Christiansen, *Nanotechnology* **19**, 295203 (2008).
6. K.Q. Peng, S.T. Lee, *Adv. Mater.* **23**, 198 (2011).
7. K.Q. Peng, Y. Xu, Y. Wu, Y.J. Yan, S.T. Lee, J. Zhu, *Small* **1**, 1062 (2005).
8. Y. Li, Q. Chen, D. He, J. Li, *Nano Energy* **7**, 10 (2014).
9. B.Z. Tian, X.L. Zheng, T.J. Kempa, Y. Fang, N.F. Yu, G.H. Yu, J.L. Huang, C.M. Lieber, *Nature* **449**, 885 (2007).
10. M. Khorasaninejad, M.M. Adachi, J. Walia, K.S. Karim, S.S. Saini, *phys. status solidi a* **210**, 373 (2013).
11. N. Fukata, K. Sato, M. Mitome, Y. Bando, T. Sekiguchi, M. Kirkham, J. Hong, Z.L. Wang, R.L. Snyder, *ACS Nano* **4**, 3807 (2010).
12. T.C. Yang, T.Y. Huang, H.C. Lee, T.J. Lin, T.J. Yen, *J. Electrochem. Soc.* **159**, B104 (2012).
13. E. Martines, K. Seunarine, H. Morgan, N. Gadegaard, C.D.W. Wilkinson, M.O. Riehle, *Nano Lett.* **5**, 2097 (2012).
14. M. Dutta, L. Thirugnanam, P.V. Trinh, N. Fukata, *ACS Nano* **9**, 6891 (2015).
15. V.T. Pham, M. Dutta, H.T. Bui, N. Fukata, *Adv. Nat. Sci.: Nanosci. Nanotechnol.* **5**, 045014 (2014).
16. Z. Huang, T. Shimizu, S. Senz, Z. Zang, N. Geyer, U. Gosele, *J. Phys. Chem. C* **114**, 10683 (2010).
17. S. Piscanec, M. Cantoro, A.C. Ferrari, J.A. Zapien, Y. Lifshitz, S.T. Lee, S. Hofmann, J. Robertson, *Phys. Rev. B* **68**, 241312 (2003).
18. N.H. Nickel, P. Lengsfeld, I. Sieber, *Phys. Rev. B* **61**, 15558 (2000).
19. Z. Huang, N. Geyer, P. Werner, J. Boor, U. Gösele, *Adv. Mater.* **23**, 285 (2011).
20. K.Q. Peng, H. Fang, J.J. Hu, Y. Wu, J. Zhu, Y.J. Yan, S.T. Lee, *Chem.-Eur. J.* **12**, 7942 (2006).
21. K. Sato, M. Dutta, N. Fukata, *Nanoscale* **6**, 6092 (2014).
22. H. Mehrer, *Diffusion in Solids: Fundamentals, Methods, Materials, Diffusion-Controlled Processes* (Springer: 2009).